RSC Advances

PAPER

View Article Online
View Journal | View Issue

Cite this: *RSC Adv.*, 2021, **11**, 19864

Dehydrocyclization–cracking of methyl oleate by Pt catalysts supported on a ZnZSM-5–Al_2O_3 hierarchical composite†

Atsushi Ishihara, * Yuu Tsuchimori and Tadanori Hashimoto

The dehydrocyclization–cracking of methyl oleate was performed by ZnZSM-5–Al_2O_3 hierarchical composite-supported Pt catalysts in the range of 450–550 °C under 0.5 MPa hydrogen pressure. Most catalysts converted methyl oleate completely and produced aromatics with more than 10 wt% yield as well as valuable fuels even at 450 °C. The reactivity of catalysts changed remarkably depending on the addition method of Pt, while supporting Pt of 0–0.16 wt% did not affect the pore structure of each catalyst. When Pt was introduced into the composite support by the conventional impregnation method, remarkable hydrocracking proceeded through the decarboxylation and decarbonylation of methyl oleate and the successive conversion of C17 fragments and gave the significant amounts of gaseous products. Nevertheless, the selectivity for the aromatics of the gasoline fraction was relatively high and the yields of aromatics reached maximum 19% at 500 °C under 0.5 MPa, suggesting that gaseous olefins would be cyclized through the Diels–Alder reaction on ZnZSM-5 in the composite support. In contrast, when Pt was introduced into catalysts by ion-exchange with ZnZSM-5, the significant conversion of methyl oleate was inhibited and produced liquid fuels in a wide range.

Received 6th April 2021
Accepted 14th May 2021

DOI: 10.1039/d1ra02677a

rsc.li/rsc-advances

1. Introduction

Although the combustion of transportation fuels discharges a large amount of CO_2, it is expected that people's consumption will continue, and can eventually lead to their shortage. Therefore, the use of renewable alternatives is necessitated and new production methods for carbon neutral transportation fuels have been developed. Liquid fats and related compounds are among the most probable candidates[1] and the esterification of fat to obtain fatty acid methyl ester (FAME) as a biodiesel oil has already been performed regionally.[2,3] It seems that, in advanced countries, the demand for transportation fuels may decrease, not only because of environmental issues but also due to the decrease in the population. The increase in the use of wind and solar energies may spur further moves in this direction toward alternative fuels. However, since the products of polymers cannot be made by these natural energies and have to be produced by carbonaceous materials, the production of polymers from renewable biomass becomes more important.[3–5] In such a situation, the production of aromatic compounds from liquid biomass, such as fats and FAMEs, using catalysts has attracted much attention and hydrocracking and catalytic cracking have become among the most important technologies since both gasoline and polymer products could include large amounts of aromatic compounds.[6–28] Especially, HZSM-5-based catalysts modified by Zn and Ga have been effective for the selective production of aromatics, such as benzene, toluene, and xylene (BTX), in the transformation of not only hydrocarbons[29] but also biomass-derived compounds.[9–16] In contrast to the cases of ZSM-5, other zeolites of β, Y, mordenite *etc.* generate less aromatics in the catalytic cracking of fat-related compounds.[16] In other reports for the conversion of fats and fat-related compounds, the addition of transition metals,[17–20] the architecture of hierarchical structures,[21] the modification of the SiO_2/Al_2O_3 ratio,[15,22] the utilization of different catalyst systems,[23–26] *etc.* have been used to promote the production of aromatic compounds. When compared to the cases of fats, however, there are few examples where FAME has been utilized for the production of aromatics.

It was proposed that the dehydrocyclization–cracking reaction of a fat could provide not only the aromatics of BTX but also hydrogen in high yields using an ideal multi-functional catalyst that has the abilities to support hydrocracking, dehydrocyclization, diffusion, and cracking simultaneously.[4,6] Multi-functional Pt/NiMo/ZnZSM-5–Al_2O_3 hierarchical composite catalysts have been used to give liquid fuel fractions of gasoline, kerosene, and gas oil, including aromatics with high yields from soybean oil. On the other hand, multi-functional ZnZSM-5–Al_2O_3 hierarchical composite catalysts also gave BTX selectively from *n*-pentane through a Diels–Alder reaction of butadiene with ethene, propene, and butenes.[29] In the course of our study, a method involving the novel direct dehydrocyclization–

Division of Chemistry for Materials, Graduate School of Engineering, Mie University, Japan. E-mail: ishihara@chem.mie-u.ac.jp

† Electronic supplementary information (ESI) available. See DOI: 10.1039/d1ra02677a

cracking of FAME, where 2 mol of aromatics and 6 mol of hydrogen from a molecule of FAME could be produced, was proposed. When it was assumed that this reaction could proceed selectively, FAME would be utilized for an energy carrier as well as a petrochemical raw material and as a reagent for gasoline blend. Although the production of hydrogen was not achieved, it was found that 20 wt% of aromatics could be produced with the use of NiMo/ZnZSM-5–Al_2O_3 hierarchical composite catalysts under less severe conditions.[30] In the present study, Pt was used as an active metal instead of NiMo and the reaction of methyl oleate was performed at a hydrogen pressure of 0.5 MPa and temperature range of 450–550 °C to investigate the effects of Pt, ZnZSM-5 and alumina on the activity and the selectivity for the products. It was found that hierarchical composite-supported Pt catalysts could convert methyl oleate effectively to aromatics under moderate conditions.

2. Materials and methods

2.1 Preparation of IO–PtZnZSM-5–Al_2O_3 and IM–Pt/ZnZSM-5–Al_2O_3 hierarchical composite catalysts

Commercially available HZSM-5 (MFI, SiO_2/Al_2O_3 (mol/mol) 24, HSZ-822HOA, Tosoh) was used. The normal ion-exchange method was used to make Zn-exchanged ZSM-5 using zinc nitrate hexahydrate. An aqueous ammonia solution was used to control the pH and the detailed method is given in the reported paper.[29] Briefly, commercial 28 wt% aqueous ammonia solution was initially diluted by about thousand-fold ion-exchanged water, and then a larger amount of NH_3 than required to neutralize the acid sites of ZSM-5 and ZnZSM-5 was dropwise added until the pH value exceeded 8. The Zn added mostly entered into ZSM-5 and the Zn content in ZnZSM-5 was quantified by X-ray fluorescence (XRF, Shimadzu EDX-720). Al_2O_3, which can be industrially used for hydrotreatment, was provided by Nippon Ketjen (average pore diameter 8 nm, pore volume 0.70 $cm^3\ g^{-1}$ and surface area 250 $m^2\ g^{-1}$). Alumina-sol (70 wt% of Al_2O_3, Cataloid AP-1, Shokubai Kasei) was used as a binder. The hierarchical composite support, ZnZSM-5–Al_2O_3, was prepared by the kneading method. The weight ratio of ZnZSM-5 : Al_2O_3 : binder after calcination was 25 : 60 : 15. These three components were mixed with water until a clay-like solid was obtained, and its calcination was performed at 500 °C for 3 h in air.[6,27] Pt of about 0.10–0.16 wt% was added to the ZnZSM-5–Al_2O_3 composite support by the conventional impregnation method using an aqueous solution of $H_2[PtCl_6]\cdot 6H_2O$. All the Pt used was supported on the composite. When Pt was added by the ion-exchange method, ZnZSM-5 and an aqueous solution of $H_2[PtCl_6]\cdot 6H_2O$ were used before kneading with Al_2O_3 and the binder. In contrast to the case of the impregnation method, only about a half of the used amount of Pt was observed in the resulting catalysts for the ion-exchange method, indicating that about a half of the Pt was not introduced into the Pt-exchangeable acid sites of ZnZSM-5, probably because the Zn, which was initially exchanged in such acid sites, inhibited the introduction of Pt sterically. The names of the catalysts prepared by the Pt ion-exchange took the form IO*x*–PtZn(*y*)ZA, where IO means the ion-exchange method, *x* is the number of the three catalyst samples in order, Pt is platinum, Zn is zinc, *y* is a molar percentage of Zn against Al atom in the ZSM-5 itself, Z means ZSM-5, and A means Al_2O_3. For the catalyst prepared by the impregnation method, IM was used instead of IO and a slash (/) was put before ZnZSM-5–Al_2O_3.

2.2 Characterization of IO–PtZnZSM-5–Al_2O_3 and IM–Pt/ZnZSM-5–Al_2O_3 hierarchical composite catalysts

XRD patterns of the catalysts were measured using a Rigaku Ultima IV system to estimate the presence of crystals. N_2 adsorption and desorption isotherms were measured using a BELSORP mini II (Microtrackbel) system to estimate the pore structures of the catalysts. The total surface area of a catalyst was calculated by the Brunauer–Emmett–Teller (BET) method. The mesoporous surface area and pore volume for pore sizes larger than 3.3 nm were calculated by the Barrett–Joyner–Halenda (BJH) method. The temperature-programmed desorption of NH_3 (NH_3-TPD) was measured by a gas chromatography–thermal conductivity detector (GC–TCD, Shimadzu GC-8A) to estimate the amount and the strength of the acid sites. Thermogravimetric–differential thermal analysis (TG–DTA) measurements were carried out to calculate the amount of coke formed using a TG–DTA (Shimadzu, DTG-60AH) system. Details of these experiments are reported elsewhere.[6,27]

2.3 Dehydrocyclization–cracking of methyl oleate by the IO–PtZnZSM-5–Al_2O_3 and IM–Pt/ZnZSM-5–Al_2O_3 hierarchical composite catalysts

Methyl oleate (guaranteed reagent (GR), Wako) was commercially available and was used for the dehydrocyclization–cracking without further purification. The catalysts were presulfided before the reaction at H_2S/H_2 at 30 cc min^{-1} and 400 °C for 3 h. After the presulfiding, the dehydrocyclization–cracking reaction was performed using a fixed-bed flow reactor (length 30 cm, inner diameter (ID) 8 mm) and 1 g of catalyst (600 to 355 μm: 70 wt%, 355 to 125 μm: 30 wt%) at a feed of 100% methyl oleate, weight hourly space velocity (WHSV) of 6.1 h^{-1}, reaction temperature of 400–550 °C, heating rate of 5 °C min^{-1}, H_2 flow rate of 300 cc min^{-1}, and H_2 pressure of 0.5 MPa. The feed was introduced to the reactor using a liquid pump (pressure resistant 3 MPa, Nihon Seimitsu Science). Liquid products were collected with a gas–liquid separator and the gaseous products were collected in a Tedlor bag through a regulator. The products were determined by a gas chromatography–flame ionization detector (GC–FID, Shimadzu GC-2014, GC-2010) and GC-TCD (Shimadzu GC-8A). First, the flow rate of gaseous products and the weight of liquid products, including water were individually measured. Gas products with C1–C4 and liquid products with C15–18 were determined by GC-FID (Shimadzu GC-2014) separately. CO and CO_2 were determined by GC–TCD (Unibeads C column, Shimadzu GC-8A). The hydrocarbon products with C5–C14 were determined by GC-FID with paraffin, olefin, naphthene, and aromatic (PONA) solution (Shimadzu GC-2010), in which more than 95% of the hydrocarbons were assigned. Details of the determination of all the products are cited elsewhere.[6,27]

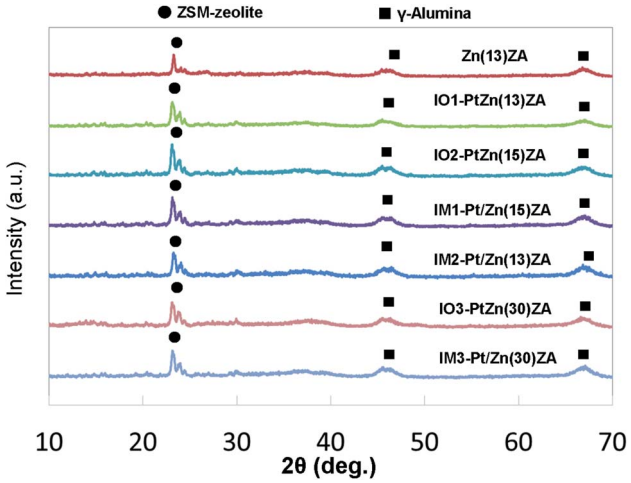

Fig. 1 XRD patterns of fresh ZnZSM-5–Al_2O_3, IO–PtZnZSM-5–Al_2O_3, and IM–Pt/ZnZSM-5–Al_2O_3 hierarchical composite catalysts. Method of Pt addition: IO = ion-exchange method; IM = impregnation method. *X* in Zn(*X*) means mol% of Zn/Al in ZSM-5. ZA means the ZSM-5–Al_2O_3 composite support.

3. Results and discussion

3.1 Characterization of the IO–PtZnZSM-5–Al_2O_3 and IM–Pt/ZnZSM-5–Al_2O_3 hierarchical composite catalysts

XRD patterns of the IO–PtZnZSM-5–Al_2O_3 and IM–Pt/ZnZSM-5–Al_2O_3 catalysts are shown in Fig. 1. Every catalyst exhibited the signals of ZSM-5 crystals with a maximum peak at 2θ of about 23°. Broad alumina signals were also observed at 2θ values of about 46° and 67°. Further, a signal of Pt was not observed, suggesting that Pt would be dispersed for both catalysts using the ion-exchange method and the impregnation method. Zn species were not detected either. Almost the same XRD patterns were observed for the catalysts after the reaction, as shown in Fig. S1.† These results are consistent with the previous results from the catalysts used in the methyl oleate, fat, and aromatics conversions.[4,6,27–32]

The pore structures of fresh IO–PtZnZSM-5–Al_2O_3 and IM–Pt/ZnZSM-5–Al_2O_3 catalysts were estimated by N_2 adsorption and desorption measurements as shown in Table 1. Zn(13)ZA, a ZnZSM-5–Al_2O_3 composite support, had a BET-surface area (SA) of 283 $m^2\ g^{-1}$, total pore volume (TPV) of 0.62 $cm^3\ g^{-1}$, BJH-SA of 292 $m^2\ g^{-1}$, BJH-PV of 0.61 $cm^3\ g^{-1}$, and BJH-pore diameter (PD) of 11 nm. The amount of Pt added in the range of 0–0.16 wt% did not affect the pore structure, and the surface areas, pore volumes, and pore diameters of the Pt-supported catalysts were almost the same as those of the Zn(13)ZA support. It seems that the effect of the amount of Zn on the surface area and pore volume would also be small. Further, values by the BJH method, which only provides information for the mesopores, were very similar to those of BET-SA and TPV, indicating that the contribution of not zeolite but alumina to the pore structure could be dominant. The results from the used catalysts are shown in Table S1† and changes in the pore structure were hardly observed, indicating that neither significant coke deposition nor the decomposition of the pore structure would have occurred by the dehydrocyclization–cracking of methyl oleate. These results agreed with those for the dehydrocyclization–cracking of soybean oil.[4,6]

Table 1 and Fig. 2 exhibit the amounts of NH_3 desorbed and the profiles by NH_3-TPD of the catalysts, respectively. When the strong acid site calculated in the range 350–650 °C was compared between the catalysts, the Pt-supported catalysts exhibited slightly higher amounts regardless of the addition method of Pt, suggesting that the addition of Pt could make the acid sites. In contrast to this, it seems that the change in the amounts of weak acid sites calculated in the range 100–350 °C was rather low, and that the incorporation of Zn decreased the strong acid sites, probably because of the neutralization of the Brønsted acid sites of ZSM-5. For example, as Zn(13)ZA included about 0.04 mmol of Zn per 1 g of catalyst and 0.32 mmol of Al in ZSM-5 per 1 g of catalyst, it is likely that a similar amount of Brønsted acid sites would decrease as Zn has the valence of +2. The amount of strong acid sites found in NH_3-TPD in the range of 350–650 °C could be regarded as Brønsted acid sites and this was 0.24 mmol in Table 1, indicating that about 25% of the Brønsted acid sites, that is 0.08 mmol, decreased with the addition of Zn. The addition of Pt increased the amount of

Table 1 Pt content, NH_3-TPD, surface area, pore volume, and average pore diameter of fresh ZnZSM-5–Al_2O_3, IO–PtZnZSM-5–Al_2O_3, and IM–Pt/ZnZSM-5–Al_2O_3 hierarchical composite catalysts

Catalyst[a]	Pt cont.[b] (wt%)	NH_3-TPD[c] 10^{-4} (mol g^{-1})	BET SA[d] ($m^2\ g^{-1}$)	Total PV[e] ($cm^3\ g^{-1}$)	Ave. PD[f] (nm)	BJH SA[d] ($m^2\ g^{-1}$)	BJH PV[e] ($cm^3\ g^{-1}$)	BJH PD[f] (nm)
Zn(13)ZA	0	6.2 (3.8/2.4)	283	0.62	8.8	292	0.61	11
IO1–PtZn(13)ZA	0.045	6.8 (4.1/2.7)	296	0.59	7.9	241	0.55	11
IO2–PtZn(15)ZA	0.090	7.0 (3.8/3.2)	291	0.65	8.9	290	0.64	11
IM1–PtZn(15)ZA	0.10	6.9 (3.8/3.1)	283	0.62	8.7	284	0.61	11
IM2–PtZn(13)ZA	0.16	7.1 (4.3/2.8)	279	0.60	8.6	281	0.59	11
IO3–PtZn(30)ZA	0.10	6.5 (4.2/2.3)	303	0.60	7.9	281	0.58	11
IM3–Pt/Zn(30)ZA	0.10	6.1 (3.8/2.3)	281	0.62	8.8	291	0.61	11

[a] Abbreviation of the sample name is the same as in the footnote of Fig. 1. [b] Pt content was determined by XRF. [c] Amounts of weak (left) and strong (right) acid sites were determined in the ranges of 100–350 °C and 350–650 °C, respectively, and are given in the parentheses. [d] Surface area. [e] Pore volume. [f] Pore diameter.

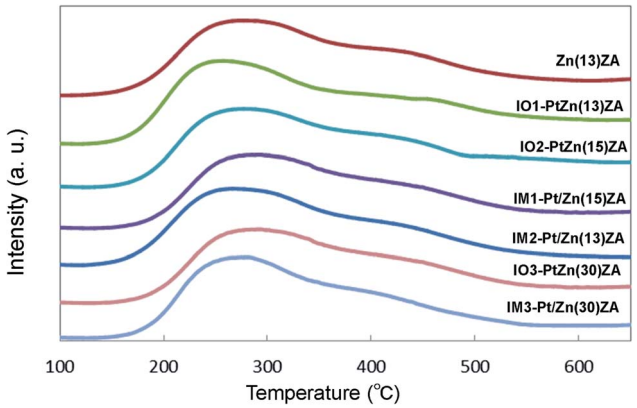

Fig. 2 NH_3-TPD curves of fresh ZnZSM-5-Al_2O_3, IO–PtZnZSM-5–Al_2O_3, and IM–Pt/ZnZSM-5–Al_2O_3 hierarchical composite catalysts. Abbreviation of the sample name is the same as in the footnote of Fig. 1.

strong acid sites of NH_3-TPD, suggesting that Pt and chloride ions would affect the acidity. Although the locations of Pt and Zn species were not measured, it is likely that Zn would be added into the inside of HZSM-5 as it was initially ion-exchanged. Further, it was difficult to add Pt species into ZSM-5 by the ion-exchange method after the addition of Zn into ZSM-5. When the impregnation method was used to add Pt species, water was removed by evaporation without filtration and thus the species would be supported on Al_2O_3 directly. On the other hand, when the ion-exchange method was used to add Pt species, the excess amount of Pt was removed by filtration and the species would be located on ZnZSM-5, although it is not known whether they would locate in the inside or the outside of ZnZSM-5.

Fig. 3a and b show TEM images of fresh IM1–Pt/ZnZSM-5–Al_2O_3 and used IM1–Pt/ZnZSM-5–Al_2O_3 hierarchical composite catalysts. The images, where zeolite crystals were surrounded by needle-like crystals of Al_2O_3 and a totally hierarchical structure was formed, were seen in both fresh and used composite catalysts. There are few differences between the images of the fresh and used catalysts. In this catalyst, Zn was exchanged initially into ZSM-5 and then Pt was added to the ZnZSM-5–Al_2O_3 composite support by the impregnation method. Therefore, it seems that Zn would be located in the inside of ZSM-5 and that Pt would be located on the surface of Al_2O_3 and the outer surface of ZSM-5, although the exact locations of Zn and Pt were not measured.

In summary, at the preparation stage of the IO method, Pt oxidative species may interact with acid sites neutralized by ammonia and be exchanged with ammonium ions. These are reduced at the reaction stage with H_2 to Pt metal species, which would be put into the acid sites of ZSM-5 finally. In contrast, most the Pt oxidative species may be put on to the Al_2O_3 surface directly after calcination at the preparation stage of the IM method and be reduced to Pt metal species at the reaction stage. Pt and Zn were found to exist very near in the ZSM-5 microporous system using the IO method, and further the reactivity of methyl oleate was significantly different between catalysts in the IO and IM methods (see Section 3.2). Although there was no relevant evidence of a strong interaction between Pt and Zn, there may be the formation of species like Pt–Zn alloy.

3.2 Dehydrocyclization–cracking of methyl oleate using ZnZSM-5–Al_2O_3, IO–PtZnZSM-5–Al_2O_3, and IM–Pt/ZnZSM-5–Al_2O_3 hierarchical composite catalysts

ZnZSM-5–Al_2O_3, IO–PtZnZSM-5–Al_2O_3, and IM–Pt/ZnZSM-5–Al_2O_3 hierarchical composite catalysts prepared by the ion-exchange and impregnation methods were used for the dehydrocyclization–cracking of methyl oleate. The results at 500 °C are shown in Table 2, Fig. 4 and 5, and those at 450 °C and 550 °C are shown in Tables S2, S3 and Fig. S2–S4.† Table 2 shows the selectivity of the products, the ratio of olefins to paraffins for the gaseous fraction (C2–C4), the ratio of iso- to normal-hydrocarbons (*iso*-/*n*-), the research octane number (RON) for gasoline (C5–C11), the cetane number of diesel oil (C15–C18) fractions, and the yield of aromatics at 500 °C. Fig. 4 exhibits the carbon number distribution of gas and liquid products. When Pt was added to the catalysts by the impregnation method, the hydrocracking to lighter hydrocarbons proceeded remarkably, suggesting that Pt/Al_2O_3 species would

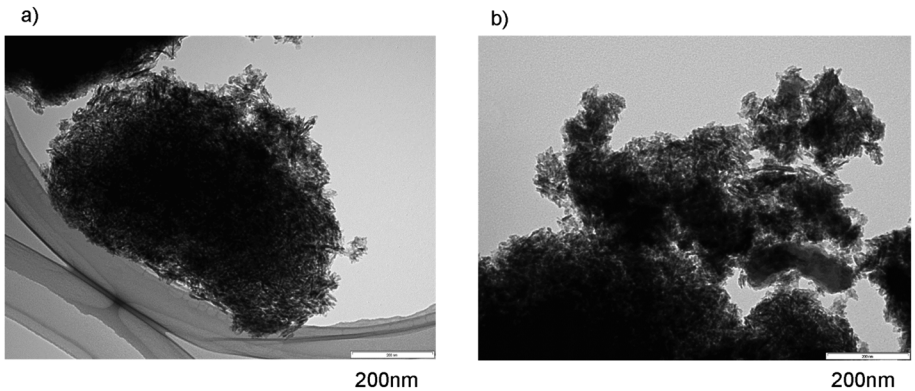

Fig. 3 TEM images of (a) fresh IM1–Pt/Zn(15)ZSM-5–Al_2O_3 and (b) used IM1–Pt/Zn(15)ZSM-5–Al_2O_3 hierarchical composite catalysts. Abbreviation of the sample name is the same as in the footnote of Fig. 1.

Table 2 Product yield, *iso*/*n* ratio, RON, cetane number, aromatic yields of ZnZSM-5–Al_2O_3, IO–PtZnZSM-5–Al_2O_3, and IM–Pt/ZnZSM-5–Al_2O_3 hierarchical composite catalysts at 500 °C

Catalyst[a]	Conv. of methyl oleate (%)	*iso*-/*n*-(C5)	Olefin/paraffin C2	Olefin/paraffin C3	Olefin/paraffin C4	RON (C5–C14)	Cetane number (C15–C18)
Zn(13)ZA	100	1.7	0.47	2.5	0.47	90	72
IO1–PtZn(13)ZA	100	1.7	1.8	1.9	8.6	75	71
IO1–PtZn(15)ZA	100	1.7	1.3	2.3	9.4	84	71
IM1–Pt/Zn(15)ZA	100	0.78	0.27	0.58	1.7	79	74
IM2–Pt/Zn(13)ZA	100	2.3	0.22	0.13	0.46	101	75
IO3–PtZn(30)ZA	100	2.1	0.2	1.1	1.5	87	72
IM3–Pt/Zn(30)ZA	100	1.4	0.67	4.2	1.0	95	72

Selectivity of Product (wt%)						Aromatic yield (wt%)	MB[b] (%)
Gas (C1–C4)	Gasoline (C5–C11)	Kerosene (C12–C14)	Diesel (C15–C18)	C19-	CO, CO_2		
32	48	3.6	8.3	1.7	6.4 (5.5)	14	97
27	47	6.1	9.0	4.4	6.7 (5.9)	12	90
34	47	4.4	6.6	3.3	5.4 (2.9)	16	97
43	33	8.4	7.1	1.5	7.0 (2.6)	19	95
66	17	1.3	2.9	1.3	11 (2.7)	14	89
40	41	3.8	7.2	3.0	5.5 (2.9)	17	92
54	28	2.7	5.1	1.1	9.4 (2.6)	18	94

[a] Abbreviation of the sample name is the same as in the footnote of Fig. 1. [b] The material balance (MB) in Table 2 is given as wt% of the sum of recovered liquid and gas products against the feed. Water is included in the liquid product.

be very active for hydrocracking of not only an ester group of methyl oleate but also the hydrocarbon fragments formed by hydrocracking of the ester group. Although CO was formed rather than CO_2, the total amounts of CO and CO_2 formed were relatively higher, indicating that the reaction would proceed through decarbonylation and decarboxylation rather than hydrodeoxygenation, which is described in the next section. On the other hand, when Pt was added by the ion-exchange method, hydrocracking was inhibited and the carbonyl group of methyl oleate was decomposed by decarboxylation to CO_2 rather than decarbonylation to CO. Therefore, their carbon number distributions were very similar to that of the catalyst without Pt, where liquid products with the C5–C18 components increased. However, the total amounts of CO and CO_2 formed were relatively lower and therefore it seems that the reaction would mainly proceed through hydrodeoxygenation. Fig. 5 exhibits the paraffin, olefin, naphthene, and aromatic (PONA) distribution in products with 5 to 14 carbon number produced at 500 °C. The use of catalysts prepared by the impregnation method and the increase in Pt and Zn contents brought about

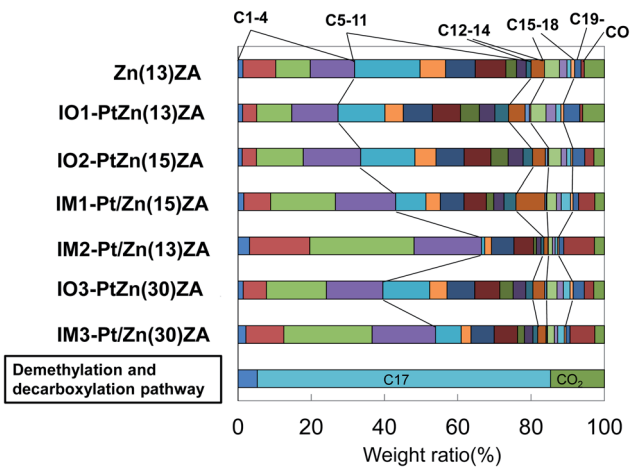

Fig. 4 Carbon number distribution of products in the dehydrocyclization–cracking of methyl oleate at 500 °C. Abbreviation of the sample name is the same as in the footnote of Fig. 1.

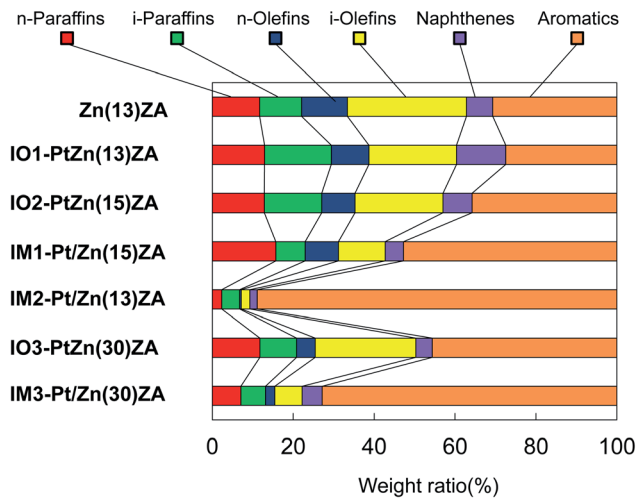

Fig. 5 PONA distribution of products in the dehydrocyclization–cracking of methyl oleate at 500 °C (C5–C14). Abbreviation of the sample name is the same as in the footnote of Fig. 1.

the increase in the selectivity for aromatic compounds with 5 to 14 carbon number, suggesting that light olefins formed by hydrocracking could appropriately be cyclized on Zn species in the inside of ZnZSM-5. This was also confirmed by the low selectivity for olefins (see Table 2 and Fig. 5) in the catalysts prepared by the impregnation. Although IM2–Pt/Zn(13)ZA exhibited the highest selectivity for aromatic compounds, the yield of aromatics was rather low because of the low selectivity for the gasoline fraction. When NiMo (NM) sulfide was supported on ZnZSM-5–Al_2O_3 (ZnZA) composites, the yield of aromatics had an optimum amount of NM contents, and the 9.3NM/ZnZA catalyst gave the highest yield of 20 wt%.[30] In the present study, IM1–Pt/Zn(15)ZA exhibited the highest aromatics yield of 19%, very near to that of this 9.3NM/ZnZA catalyst. When the dehydrocyclization–cracking of a fat was performed using the catalysts with both Pt and NiMo at higher than 500 °C, significant aromatics yields of more than 10% were obtained. At 500 °C and lower, and without the addition of Pt metal to the composite-supported NiMo catalysts, the aromatics yields were rather low.[4,32] In the present study, IO–PtZnZA and IM–Pt/ZnZA catalysts could be used for the conversion of methyl oleate and gave significant amounts of aromatics. The selectivity of C5–C18 fractions for IO1–PtZn(13)ZA was the highest at 62% at 500 °C.

For other temperatures than 500 °C, the aromatics yields at 450 °C were somewhat lower, while those at 550 °C were higher than 15% for most the catalysts. The selectivities for the C5–C18 fractions for Zn(13)ZA without Pt and IO2–PtZn(15)ZA reached 72% and 66%, respectively, at 450 °C, although the fraction with more than C18 (C19-) tended to increase. To yield the larger amount of aromatics at as low a temperature as 500 °C and as low a pressure as 0.5 MPa, the most suitable combination of Pt/Al_2O_3 and ZnZSM-5 may be necessary as exhibited in IM1–Pt/Zn(15)ZA. It seems that only ZnZA could not increase the yield of aromatics and that only Pt/Al_2O_3 could not convert methyl oleate to liquid fuel fractions. These result suggested that more fine tuning might be needed to increase the aromatics from the dehydrocyclization of hydrocarbon fragments.

The composite support was composed of ZnZSM-5 and Al_2O_3 by about a 1 : 3 weight ratio, including the binder of Al_2O_3. It seems that Pt species in the IM method would encounter, interact with, and be physically adsorbed on ZnZSM-5 and Al_2O_3 by the possibility near 1 : 3. Pt species initially put on the composite may exist at the same place or near during calcination and react upon changing the size and the oxidation state of the Pt species. In contrast to the IM method, Pt species in the IO method would exist near ZnZSM-5 during the reaction. The difference in the location of Pt species also leads to a difference between the reactivities of the catalysts prepared by the IO and IM methods.

It seems that the structure of the composite supports would not be changed by the location of Pt, while the reactivity of Pt would be changed by its location. Hydrocracking reactivity was generated by Pt species supported on Al_2O_3 in the IM method while it was inhibited on Pt species near ZnZSM-5 in the IO method, probably because of the narrow space around Pt in microporous ZnZSM-5 and the concentration of Pt near ZnZSM-5.

Table 3 summaries the results from the measurement of coke formation by TG–DTA using the ZnZA, IO–PtZnZA, and IM–Pt/ZnZA composite catalysts. When Pt was added by the impregnation method, the coke formation in the range of 400–600 °C was rather low for the IM1– and IM2–Pt/ZnZA catalysts, indicating that Pt/Al_2O_3 plays a very important role to convert the basic structure of methyl oleate. Using ZnZA without Pt and IO1–PtZnZA with a low Pt content, larger amounts of coke were observed in the range of 400–600 °C, indicating that, as Pt does not exist on Al_2O_3, significant coke formation would occur. In the present study, although the effect of the ZnZSM-5 content was not examined, it was reported that, as the ZnZSM-5 content was smaller, significant coke formation would occur.[29] These results suggested that the coke could mainly be generated in the hydrocracking of the ester structure in methyl oleate. In the present study, the catalysts without Pt on Al_2O_3 tended to form a larger amount of coke, especially in the range of 400–600 °C, compared to the catalysts by Pt impregnation. This result also suggested that the direct addition of Pt on the Al_2O_3 support could appropriately hydrocrack methyl oleate and inhibit the formation of coke that is difficult to remove at a hydrogen pressure of 0.5 MPa. Although it has been reported that not only NiMo but also Pt are needed for the conversion of fat,[4,6] it was found in this study that NiMo or Pt could be used to decompose methyl oleate, as one FAME, by activating hydrogen.

Table 3 Analysis of coke formation by TG–DTA measurement of the used ZnZSM-5–Al_2O_3, IO–PtZnZSM-5–Al_2O_3, and IM–Pt/ZnZSM-5–Al_2O_3 hierarchical composite catalysts

Catalysts[a]	200–300 °C	300–400 °C	400–500 °C	500–600 °C	Total[b] (mg)
Zn(13)ZA	0.02	0.01	0.86	1.96	2.84 (2.81)
IO1–PtZn(13)ZA	0.04	0.32	0.99	2.21	3.56 (3.20)
IO1–PtZn(15)ZA	0.04	0.37	0.93	1.57	2.88 (2.47)
IM1–Pt/Zn(15)ZA	0.10	0.20	0.77	1.34	2.41 (2.11)
IM2–Pt/Zn(13)ZA	0.32	0.46	0.83	1.30	2.91 (2.09)
IO3–PtZn(30)ZA	0.05	0.24	1.03	1.55	2.88 (2.59)
IM3–Pt/Zn(30)ZA	0.05	0.15	0.89	1.74	2.84 (2.64)

[a] Abbreviation of the sample name is the same as in the footnote of Fig. 1. [b] Values in the range 400–600 °C are given in parentheses.

The dehydrocyclization–cracking reaction includes the hydrocracking of ester, the hydrocracking and cracking of alkyl fractions, and the dehydrogenation and cyclization of olefinic hydrocarbons simultaneously. Therefore, exact activation energies could not be estimated. In the reaction range of 450–550 °C, where 100% methyl oleate was converted, the aromatics formation was favorable according to equilibrium theory.[33] On the other hand, we already reported that the aromatics formation was affected by both the temperature and the presence of matrix alumina in the dehydrocyclization of *n*-pentane.[34] These results suggested that even a small molecule like *n*-pentane would influence the aromatics formation at this temperature range by diffusion control as well as by kinetic control. In the present study, a higher temperature was selected in order to obtain aromatics with a higher yield. With increasing the temperature from 450 °C to 500 °C, the aromatics yields increased for most of the catalysts. However, with increasing the temperature from 500 °C to 550 °C, the aromatics yields were

similar, suggesting that, as cracking to stable gaseous alkane is also favored at higher temperature, the aromatics yields would not increase so much.

3.3 Reaction pathways in the dehydrocyclization–cracking of methyl oleate using the IO–PtZnZSM-5–Al_2O_3, and IM–Pt/ZnZSM-5–Al_2O_3 hierarchical composite catalysts

Possible reaction pathways for the formation of aromatics from methyl oleate using the IO–PtZnZSM-5–Al_2O_3 and IM–Pt/ZnZSM-5–Al_2O_3 hierarchical composite catalysts are shown in Fig. 6. Although decarboxylation, decarbonylation, and hydrodeoxygenation proceeded competitively for all the catalysts, it seemed that the Pt/Al_2O_3 part in IM–Pt/ZnZSM-5–Al_2O_3 would mainly catalyze decarboxylation and decarbonylation to produce CO_2 and CO, respectively, with hydrocarbon fragments of C17 and C18. The hydrocarbon fragments would be further hydrocracked by Pt/Al_2O_3 to C2–C15 alkanes, which may be dehydrogenated to C2–C15 alkenes on metallic sites of Pt or Zn. The hydrocarbon fragments could also be cracked by acid sites in ZnZSM-5 part forming C2–C15 alkenes. The C2–C8 hydrocarbons formed would be cyclized to aromatics on ZnZSM-5. However, the reaction routes might be different depending on the addition method of Pt species. When Pt was added by the impregnation method on a hierarchical composite, significant amounts of olefins in the produced gaseous hydrocarbons would be cyclized to aromatics through Diels–Alder reactions in the inside of ZnZSM-5.[29] ZnZSM-5 was considered to have small pore mouths because even Pt was difficult to be incorporated into ZnZSM-5 by the ion-exchange method. Therefore, only gaseous hydrocarbons could be introduced into the inside of ZnZSM-5. It is likely that, in the catalyst prepared by the impregnation of Pt, olefins with C2–C4 would be formed first and would then be cyclized to generate BTX. It was reported that olefins with C2–C4 produced by cracking would be cyclized through a Diels–Alder cyclization in active Zn species in the dehydrocyclization of *n*-pentane.[29] In that study, it was demonstrated that the reactions of ethylene and C4 olefin, propylene and C4 olefin, and two molecules of C4 olefins could generate the target benzene, toluene, and xylene, respectively.[29] The result could support the aromatization route I shown in Fig. 6. In contrast to this, it seems that hydrocarbons with C6–C8 would be cyclized on the outside of PtZnZSM-5 for the catalysts prepared by Pt ion-exchange with ZnZSM-5 in aromatization route II. This mechanism was proposed for the dehydrocyclization–cracking reaction of fat using the β-zeolite-Al_2O_3 hierarchical composite-supported PtNiMo sulfide catalysts.[4] Although the β-zeolite-containing Al_2O_3-hierarchical composite-supported Pt/NiMo catalysts did not form a lot of gaseous products, significant amounts of aromatics were produced in the dehydrocyclization–cracking of soybean oil. When Pt was added by the impregnation method, aromatics were formed simultaneously with the significant production of gaseous products. For the catalysts prepared by the Pt ion-exchange method, however, the selectivity for gaseous hydrocarbons were rather low, and the hydrocarbon products may find it difficult to enter in to the inside of PtZnZSM-5. C6–C8 hydrocarbons would be cyclized to BTX on the outside of PtZnZSM-5 before entering in to its inside.

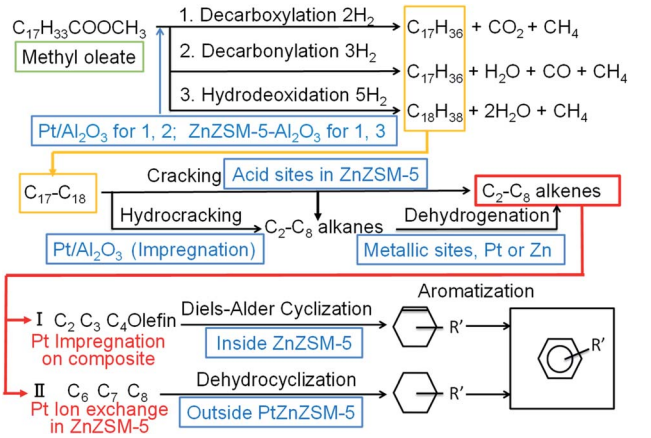

Fig. 6 Reaction pathways in the dehydrocyclization–cracking of methyl oleate by IO–PtZnZSM-5–Al_2O_3 and IM–Pt/ZnZSM-5–Al_2O_3 hierarchical composite catalysts.

Zeolite-supported Pt catalysts have not been used for the cracking and hydrocracking of a fat and FAME. The combination of Pt/zeolite with NiMo/Al_2O_3 was reported for diesel fuel production at a 5 MPa hydrogen pressure and higher.[35] Our group reported the dehydrocyclization–cracking of soybean oil for aromatics production catalyzed by Pt/NiMo/zeolite-Al_2O_3 hierarchical composite systems.[4,6,32] In order to treat soybean oil at as low a pressure as 1 MPa, not only NiMo sulfides but also Pt metal were needed. On the other hand, methyl oleate could be treated using only NiMo sulfides without Pt at as low a pressure as 0.5 MPa. In the present study, it was reported for the first time that zeolite-Al_2O_3 hierarchical composite-supported Pt catalysts could also be used to treat methyl oleate at as low a pressure as 0.5 MPa. There are very few examples in which FAME, such as methyl oleate, could be treated to obtain chemicals and fuels at as low a hydrogen pressure as 0.5 MPa. Although the conversion of FAME and the selectivity for alkanes with C5–C18 over Ni/HZSM-5 at 280 °C and H_2 0.8 MPa reached 85% and 88%, respectively,[17] the conversion decreased significantly after 3 days because of the carbon deposition. In the hydrocracking of methyl oleate using NiMo/Al_2O_3 and Ni–La/Zn-ZSM-5–Al_2O_3 at H_2 50–90 bar and 400–445 °C,[11] BTX was mainly obtained. FAME was hydrocracked over mordenite-supported Ni, Co, and Mo catalysts at 400 °C to obtain liquid fuels.[18] Ni-supported mesoporous Y zeolite was suitable for this reaction and gave a high selectivity of jet fuel alkanes from light microalgal biodiesel.[21] In that study, it was proposed that most the fatty acids could be deoxygenated first to C15–C16 by decarboxylation and decarbonylation, and then cracking of the long-chained alkane occurred to form short alkanes and aromatics. Some results in that study would agree with the reaction routes proposed in the present study.

Apart from a biomass-derived feed, systems including Pt and Zn/or Ga/ZSM-5 have been reported in the transformation of light alkanes.[36,37] It has already been known for a long term that Pt-ZSM-5-based catalysts are less effective for the aromatization

of light alkanes than Ga- or Zn-ZSM-5-based catalysts because undesirable hydrocracking and olefins hydrogenation proceed on the Pt surface, which would lead to the formation of unreactive CH_4 and C_2H_6.[36] Therefore, it was proposed that the drawbacks could be inhibited by alloying with Pt and by raising the temperature. Ellouh *et al.* reported that light paraffinic naphtha with C5 and C6 could be converted at 550 °C into BTX in high yields using Pt–Zn or Ga/ZSM-5 made by the wet-impregnation method.[38] Matsuoka *et al.* reported that light alkanes with C2–C5 could be converted to aromatics using polyfunctional metallosilicate catalysts with Pt, Zn, or Ga.[39] When Pt was added into the gel in the preparation of the silicate, the effect of Pt was weaker than that for Pt ion-exchanged silicate. In our present study, the effect of Pt was weaker for the catalyst prepared by the ion-exchange method than the catalyst prepared by the impregnation method, indicating that the appropriate deposition of Pt on the support surface is important for drawing the effect of Pt when the inside of ZSM-5 is crowded by another metal, for example Zn. It was also reported that, when Pt–Zn nanoparticles were supported on ZSM-5, *n*-octane was converted to *i*-octane and BTX in high selectivity because of a bimetallic–support interaction.[40] This result would be related to our results from the Pt catalyst by the ion-exchange method, where there may be an interaction of Pt with Zn, leading to the formation of BTX without the significant formation of gaseous hydrocarbons.

Although the stability was not examined, normally the hydrotreating catalyst can be used again after calcination and presulfiding processes. Under severe hydrothermal conditions, not only zeolite but also alumina is degraded. Further, it is also known that zeolite is degraded in the presence of steam in the catalytic cracking process. Further, the hydrotreatment of fat and FAME could produce water, which may degrade the catalysts. The used catalysts in the present study did not show any significant degradation as shown in the N_2 adsorption and desorption (Table S1†) and XRD (Fig. S1†) measurements of the used catalysts, indicating that the catalysts prepared would be stable at least during a short reaction time.

4. Conclusions

Methyl oleate, one of the FAME compounds, was transformed by dehydrocyclization–cracking into gaseous and liquid products using hierarchically structured ZnZSM-5–Al_2O_3 composite-supported Pt catalysts at 0.5 MPa hydrogen pressure in the range 450–550 °C. The conversions of all the catalysts reached almost 100% even at 450 °C, while the selectivity of products changed with changing the temperature. Further, the reactivity of the catalysts largely changed depending on the method used for the introduction of Pt into the catalysts. When Pt was introduced into ZnZSM-5 initially by the ion-exchange method, the production of gaseous products was inhibited while significant amounts of aromatics were obtained. When Pt was introduced into ZnZSM-5–Al_2O_3 hierarchical composites by the impregnation method, remarkable hydrocracking proceeded forming large amounts of gaseous products while aromatics were also produced significantly. IM1–Pt/Zn(15)ZA prepared by the impregnation method exhibited the highest aromatics yields of 19% at 500 °C and 550 °C. It seems that Pt species supported on Al_2O_3 would convert an ester group of methyl oleate through decarboxylation and decarbonylation, while PtZnZA would also convert it through hydrodeoxygenation as well as decarboxylation. The ester group would be transformed in to aliphatic hydrocarbons with C17 and C18, which could further be converted to lower alkenes through cracking on ZnZSM-5 and lower alkanes through hydrocracking on Pt/Al_2O_3. The final reaction pathway to produce aromatics would be different between catalysts prepared by the ion-exchange method and the impregnation method. It seems that aromatics would be formed through the cyclization of liquid hydrocarbon fragments on the outside of PtZnZSM-5 in the Pt ion-exchanged catalysts, while the formed gaseous olefins would be cyclized through Diels–Alder reactions forming aromatics in the inside of ZnZSM-5 in the Pt-impregnated catalysts.

Author contributions

Atsushi Ishihara: conceptualization; data curation; investigation; formal analysis; methodology; project administration; supervision; validation; writing original draft; writing – review & editing. Yuu Tsuchimori: writing original draft, investigation. Tadanori Hashimoto: writing – review & editing, formal analysis.

Conflicts of interest

The authors have no competing interests to declare.

Acknowledgements

The authors thank Mr Atsuki Niimi for his helpful work.

References

1 D. Kubicka, I. Kubickova and J. Cejka, Application of Molecular Sieves in Transformations of Biomass and Biomass-Derived Feedstocks, *Catal. Rev.: Sci. Eng.*, 2013, **55**(1), 1–78, DOI: 10.1080/01614940.2012.685811.

2 M. Gousi, C. Andriopoulou, K. Bourikas, S. Ladas, M. Sotiriou, C. Kordulis and A. Lycourghiotis, Processing biomass in conventional oil refineries: Production of high quality diesel by hydrotreating vegetable oils in heavy vacuum oil mixtures, *Appl. Catal., A*, 2017, **536**, 45–56.

3 A. E. Coumans and E. J. M. Hensen, A model compound (methyl oleate, oleic acid, triolein) study oftriglycerides hydrodeoxygenation over alumina-supported NiMosulfide, *Appl. Catal., B*, 2017, **201**, 290–301.

4 Y. Shirasaki, H. Nasu, T. Hashimoto and A. Ishihara, Effects of types of zeolite and oxide and preparation methods on dehydrocyclization-cracking of soybean oil using hierarchical zeolite-oxide composite-supported Pt/NiMo sulfided catalysts, *Fuel Process. Technol.*, 2019, **194**, 106109, DOI: 10.1016/j.fuproc.2019.05.032.

5 T. Kabe, A. Ishihara and W. H. Qian, *Hydrodesulfurization and Hydrodenitrogenation*, Wiley-VCH' Kodansha-Scientific, 1999.

6 A. Ishihara, R. Ishida, T. Ogiyama, H. Nasu and T. Hashimoto, Dehydrocyclization-cracking reaction of soybean oil using zeolite-metal oxide composite-supported PtNiMo sulfided catalysts, *Fuel Process. Technol.*, 2017, **161**, 17–22, DOI: 10.1016/j.fuproc.2017.02.028.

7 Y. Zheng, F. Wang, X. Yang, Y. Huang, C. Liu, Z. Zheng and J. Gua, Study on aromatics production *via* the catalytic pyrolysis vapor upgrading of biomass using metal-loaded modified H-ZSM-5, *J. Anal. Appl. Pyrolysis*, 2017, **126**, 169–179.

8 Q. Ouyang, J. Yao, N. Yang, Y. Wang, M. Yao and X. Liu, 0.7 wt% Pt/beta-Al_2O_3 as a highly efficient catalyst for the hydrodeoxygenation of FAMEs to diesel-range alkanes, *Catal. Commun.*, 2019, **120**, 46–50.

9 A. A. Taromi and S. Kaliaguine, Green diesel production *via* continuous hydrotreatment of triglycerides over mesostructured γ-alumina supported NiMo/CoMo catalysts, *Fuel Process. Technol.*, 2018, **171**, 20–30.

10 O. Singh, A. Agrawal, T. Selvaraj, I. K. Ghosh, B. P. Vempatapu, B. Viswanathan, R. Bal and B. Sarkar, Renewable Aromatics from Tree-Borne Oils (nonedible seed oil) over Zeolite Catalysts Promoted by Transition Metals, *ACS Appl. Mater. Interfaces*, 2020, **12**(22), 24756–24766, DOI: 10.1021/acsami.0c04149.

11 C. Dusescu, T. Juganaru, D. Bombos, O. Mihai and D. Popovici, Multilayered catalysts for fatty acid ester hydrotreatment into fuel range hydrocarbons, *C. R. Chim.*, 2018, **21**(3–4), 288–302, DOI: 10.1016/j.crci.2017.06.006.

12 A. Bayat and S. M. Sadrameli, Production of renewable aromatic hydrocarbons *via* conversion of canola oil methyl ester (CME) over zinc promoted HZSM-5 catalysts, *Renewable Energy*, 2017, **106**, 62–67, DOI: 10.1016/j.renene.2017.01.014.

13 E. V. Fufachev, B. M. Weckhuysen and P. C. A. Bruijnincx, Tandem catalytic aromatization of volatile fatty acids, *Green Chem.*, 2020, **22**(10), 3229–3238, DOI: 10.1039/d0gc00964d.

14 S. Tamiyakul, S. Anutamjarikun and S. Jongpatiwut, The effect of Ga and Zn over HZSM-5 on the transformation of palm fatty acid distillate (PFAD) to aromatics, *Catal. Commun.*, 2016, **74**, 49–54, DOI: 10.1016/j.catcom.2015.11.002.

15 A. Bayat, S. M. Sadrameli and J. Towfighi, Production of green aromatics *via* catalytic cracking of Canola Oil Methyl Ester (CME) using HZSM-5 catalyst with different Si/Al ratios, *Fuel*, 2016, **180**, 244–255, DOI: 10.1016/j.fuel.2016.03.086.

16 H. K. G. Singh, S. Yusup, A. T. Quitain, T. Kida, M. Sasaki, K. W. Cheah and M. Ameen, Production of gasoline range hydrocarbons from catalytic cracking of linoleic acid over various acidic zeolite catalysts, *Environ. Sci. Pollut. Res.*, 2019, **26**(33), 34039–34046, DOI: 10.1007/s11356-018-3223-4.

17 L. Chen, H. Li, J. Fu, C. Miao, P. Lv and Z. Yuan, Catalytic hydroprocessing of fatty acid methyl esters to renewable alkane fuels over Ni/HZSM-5 catalyst, *Catal. Today*, 2016, **259**(part 2), 266–276, DOI: 10.1016/j.cattod.2015.08.023.

18 J. L. Sihombing, A. N. Pulungan, M. Zubir, Jasmidi, A. A. Wibowo, S. Gea, B. Wirjosentono and Y. A. Hutapea, Conversion of methyl ester fatty acid from rice bran oil into fuel fraction *via* hydrocracking reaction over zeolite catalyst supported of Ni, Co and Mo metals, *Rasayan J. Chem.*, 2019, **12**(1), 205–213, DOI: 10.31788/rjc.2019.1215036.

19 F. Long, Q. Zhai, P. Liu, X. Cao, X. Jiang, F. Wang, L. Wei, C. Liu, J. Jiang and J. Xu, Catalytic conversion of triglycerides by metal-based catalysts and subsequent modification of molecular structure by ZSM-5 and Raney Ni for the production of high-value biofuel, *Renewable Energy*, 2020, **157**, 1072–1080, DOI: 10.1016/j.renene.2020.05.117.

20 G. Xu, C. Jia, Z. Shi, R. Liang, C. Wu, H. Liu, C. Yan, J. Fan, H. Hou and T. Ding, Enhanced catalytic conversion of camelina oil to hydrocarbon fuels over Ni-MCM-41 catalysts, *Sci. Adv. Mater.*, 2020, **12**(2), 304–311, DOI: 10.1166/sam.2020.3714.

21 T. Li, J. Cheng, X. Zhang, J. Liu, R. Huang and J. Zhou, Jet range hydrocarbons converted from microalgal biodiesel over mesoporous zeolite-based catalysts, *Int. J. Hydrogen Energy*, 2018, **43**(21), 9988–9993, DOI: 10.1016/j.ijhydene.2018.04.078.

22 S. Vichaphund, P. Wimuktiwan, V. Sricharoenchaikul and D. Atong, In situ catalytic pyrolysis of Jatropha wastes using ZSM-5 from hydrothermal alkaline fusion of fly ash, *J. Anal. Appl. Pyrolysis*, 2019, **139**, 156–166, DOI: 10.1016/j.jaap.2019.01.020.

23 Z. Yu, L. Jiang, Y. Wang, Y. Li, L. Ke, Q. Yang, Y. Peng, J. Xu, L. Dai, Q. Wu, Y. Liu, R. Ruan, D. Xia and L. Jiang, Catalytic pyrolysis of woody oil over SiC foam-MCM41 catalyst for aromatic-rich bio-oil production in a dual microwave system, *J. Cleaner Prod.*, 2020, **255**, 120179, DOI: 10.1016/j.jclepro.2020.120179.

24 Z. Zheng, J. Wang, Y. Wei, X. Liu, F. Yu and J. Ji, Effect of La-Fe/Si-MCM-41 catalysts and CaO additive on catalytic cracking of soybean oil for biofuel with low aromatics, *J. Anal. Appl. Pyrolysis*, 2019, **143**, 104693, DOI: 10.1016/j.jaap.2019.104693.

25 P. V. Lipin, O. V. Potapenko, T. P. Sorokina and V. P. Doronin, Key Features of Cotransformation of Vacuum Gas Oils and Vegetable Oils on Dual-Zeolite Cracking Catalysts, *Pet. Chem.*, 2019, **59**(7), 657–665, DOI: 10.1134/s0965544119070090.

26 C. Freitas, M. Pereira, D. Souza, N. Fonseca, E. Sales, R. Frety, C. Felix, A. Azevedo Jr and S. Brandao, Thermal and catalytic pyrolysis of dodecanoic acid on SAPO-5 and Al-MCM-41 catalysts, *Catalysts*, 2019, **9**(5), 418, DOI: 10.3390/catal9050418.

27 A. Ishihara, N. Fukui, H. Nasu and T. Hashimoto, "Hydrocracking of soybean oil using zeolite–alumina composite supported NiMo catalysts", *Fuel*, 2014, **134**, 611–617.

28 A. Ishihara, D. Kawaraya, T. Sonthisawate, K. Kimura, T. Hashimoto and H. Nasu, Catalytic cracking of soybean oil by hierarchical zeolite containing mesoporous silica-aluminas using a Curie point pyrolyzer, *J. Mol. Catal. A: Chem.*, 2015, **396**, 310–318.

29 A. Ishihara, K. Takai, T. Hashimoto and H. Nasu, Effects of a Matrix on Formation of Aromatic Compounds by Dehydrocyclization of n-Pentane Using ZnZSM-5−Al_2O_3 Composite Catalysts, *ACS Omega*, 2020, **5**, 11160–11166, DOI: 10.1021/acsomega.0c01147.

30 A. Ishihara, K. Takemoto and T. Hashimoto, Aromatics formation by dehydrocyclization-cracking of methyl oleate using ZnZSM-5-alumina composite-supported NiMo sulfide catalysts, *Fuel*, 2021, **289**, 119885.

31 A. Ishihara, T. Itoh, T. Doi, H. Nasu and T. Hashimoto, Hydrocracking of 1-methylnaphthalene/decahydronaphthalene mixture catalyzed by zeolite-alumina composite supported NiMo catalysts, *Fuel Process. Technol.*, 2013, **116**, 222–227.

32 A. Ishihara, S. Kanamori and T. Hashimoto, Effects of Zn Addition into ZSM-5 Zeolite on Dehydrocyclization-Cracking of Soybean Oil Using Hierarchical Zeolite-Al_2O_3 Composite-Supported Pt/NiMo Sulfided Catalysts, *ACS Omega*, 2021, **6**(8), 5509–5517, DOI: 10.1021/acsomega.0c05855.

33 B. C. Gates, J. R. Katzer and G. C. A. Schuit, *Chemistry of Catalytic Process, Catalytic reforming*, McGraw-Hill, 1979, ch. 3.

34 A. Ishihara, Y. Kodama and T. Hashimoto, Effect of matrix on aromatics production by cracking and dehydrocyclization of n-pentane using Ga ion-exchanged ZSM-5-alumina composite catalysts, *Fuel Process. Technol.*, 2021, **213**, 106679.

35 R. Sotelo-Boyas, Y. Liu and T. Minowa, Renewable diesel production from the hydrotreating of rapeseed oil with Pt/Zeolite and NiMo/Al_2O_3catalysts, *Ind. Eng. Chem. Res.*, 2011, **50**(5), 2791–2799, DOI: 10.1021/ie100824d.

36 P. Meriaudeau and C. Naccache, Dehydrocyclization of alkanes over zeolite-supported metal catalysts: monofunctional or bifunctional route, *Catal. Rev. - Sci. Eng.*, 1997, **39**(1 & 2), 5–48, DOI: 10.1080/01614949708006467.

37 P. L. De Cola, R. Glaeser and J. Weitkamp, Non-oxidative propane dehydrogenation over Pt-Zn-containing zeolites, *Appl. Catal., A*, 2006, **306**, 85–97, DOI: 10.1016/j.apcata.2006.03.028.

38 M. Ellouh, Z. S. Qureshi, A. Aitani, M. N. Akhtar, Y. Jin, O. Koseoglu and H. Alasiri, Light Paraffinic Naphtha to BTX Aromatics over Metal-Modified Pt/ZSM-5, *ChemistrySelect*, 2020, **5**(44), 13807–13813, DOI: 10.1002/slct.202003492.

39 A. Matsuoka, J.-B. Kim and T. Inui, Selectivity improvement in the aromatization of C2-C5 alkanes using polyfunctional metallosilicate catalysts, *Microporous Mesoporous Mater.*, 2000, **35–36**, 89–98, DOI: 10.1016/S1387-1811(99)00210-3.

40 J. S. Jarvis, J. H. Harrhy, P. He, A. Wang, L. Liu and H. Song, Highly selective aromatization and isomerization of *n*-alkanes from bimetallic Pt-Zn nanoparticles supported on a uniform aluminosilicate, *Chem. Commun.*, 2019, **55**(23), 3355–3358, DOI: 10.1039/c9cc00338j.